NIH Public Access
Author Manuscript
Neuron. Author manuscript; available in PMC 2010 September 24.

Published in final edited form as:
Neuron. 2009 September 24; 63(6): 818–829. doi:10.1016/j.neuron.2009.08.010.

High affinity kainate receptor subunits are necessary for ionotropic but not metabotropic signaling

Herman B. Fernandes[1], **Justin S. Catches**[1], **Ronald S. Petralia**[2], **Bryan A. Copits**[3], **Jian Xu**[1], **Theron A. Russell**[1], **Geoffrey T. Swanson**[3], and **Anis Contractor**[1]

[1]Department of Physiology, Northwestern University School of Medicine, 303 E Chicago Ave, Chicago, IL 60611 USA

[2]Laboratory of Neurochemistry, National Institute on Deafness and Other Communication Disorders, National Institutes of Health, Bethesda, MD 20892

[3]Department of Molecular Pharmacology and Biological Chemistry, Northwestern University School of Medicine, 303 E Chicago Ave, Chicago, IL 60611 USA

Summary

Kainate receptors are atypical members of the glutamate receptor family which are able to signal through both ionotropic and metabotropic pathways. Of the five individual kainate receptor subunits the high-affinity subunits, GluK4 (KA1) and GluK5 (KA2), are unique in that they do not form functional homomeric receptors in recombinant expression systems, but combine with the primary subunits GluK1-3 (GluR5-7) to form heteromeric assemblies. Here we generated a GluK4 mutant mouse by disrupting the *Grik4* gene locus. We found that loss of the GluK4 subunit leads to a significant reduction in synaptic kainate receptor currents. Moreover, ablation of both high-affinity subunits in GluK4/GluK5 double knockout mice leads to a complete loss of pre- and postsynaptic ionotropic function of synaptic kainate receptors. The principal subunits remain at the synaptic plasma membrane, but are distributed away from postsynaptic densities and presynaptic active zones. There is also an alteration in the properties of the remaining kainate receptors, as kainic acid application fails to elicit responses in GluK4/GluK5 knockout neurons. Despite the lack of detectable ionotropic synaptic receptors, the kainate receptor-mediated inhibition of the slow afterhyperpolarization current (I_{sAHP}), which is dependent on metabotropic pathways, was intact in GluK4/GluK5 knockout mice. These results uncover a previously unknown critical role for the high-affinity kainate receptor subunits as obligatory components of ionotropic kainate receptor function, and further, demonstrate that kainate receptor participation in metabotropic signaling pathways does not require their classic role as ion channels.

Keywords

Kainate receptors; hippocampus; mossy fiber; presynaptic; metabotropic; afterhyperpolarization; glutamate receptors

© 2009 Elsevier Inc. All rights reserved.

Correspondence: Anis Contractor Dept of Physiology Northwestern University School of Medicine 303 E. Chicago Ave Chicago, Il 60611 a-contractor@northwestern.edu Tel: 312 503 1843 Fax: 312 503 5101.

Publisher's Disclaimer: This is a PDF file of an unedited manuscript that has been accepted for publication. As a service to our customers we are providing this early version of the manuscript. The manuscript will undergo copyediting, typesetting, and review of the resulting proof before it is published in its final citable form. Please note that during the production process errors may be discovered which could affect the content, and all legal disclaimers that apply to the journal pertain.

NIH-PA Author Manuscript
NIH-PA Author Manuscript
NIH-PA Author Manuscript

NIH-PA Author Manuscript

NIH-PA Author Manuscript

NIH-PA Author Manuscript

Introduction

Kainate receptors are glutamate-gated ion channels that have complex and diverse roles in regulating synaptic transmission and cellular excitability. Five separate genes (*Grik*1-5) encode the different receptor subunits, which are categorized into two separate groups based upon their ability to form functional homomeric receptors, and their similar primary sequence homology. The principal subunits, GluK1, GluK2 and GluK3 (previously termed GluR5, GluR6 and GluR7), form functional plasma membrane-localized receptors in recombinant expression systems. GluK4 (KA1) and GluK5 (KA2) subunits are often termed the "high-affinity" subunits, because of their low nanomolar affinity for the marine toxin kainic acid, or "auxiliary" subunits, because they do not assemble as functional homomeric receptors. Instead, they modify the biophysical function and pharmacological properties of kainate receptors when co-expressed with GluK1-3 subunits (Herb et al., 1992; Werner et al., 1991).

Neuronal kainate receptors are composed of heteromeric assemblies of principal and auxiliary subunits. The unique physiological and pharmacological properties displayed by neuronal kainate receptors are determined largely by their subunit composition. Therefore, kainate receptor subunit expression in distinct neuronal cell types is an important indicator of the functional contribution of these receptors to synaptic signaling. The primary subunits are expressed in complex patterns during development and in the adult brain (Bahn et al., 1994; Wisden and Seeburg, 1993). In some neurons a single principal subunit determines the presence of functional plasma membrane kainate receptors (Mulle et al., 1998), whereas in other neuronal cell types kainate receptors are comprised of multiple primary subunits (Mulle et al., 2000). In contrast the high-affinity subunits display two very distinct expression profiles. The GluK5 subunit is expressed ubiquitously in nearly all neuronal populations, suggesting that it is a constituent of most heteromeric neuronal kainate receptor assemblies (Herb et al., 1992). The GluK4 subunit shows very limited and well-defined expression in just a few neuronal cell types after birth (Bahn et al., 1994; Kask et al., 2000). In the hippocampus GluK4 mRNA is expressed at high levels in the CA3 pyramidal neurons and at very low levels in granule cells in the dentate gyrus (Werner et al., 1991). In all other neurons in the hippocampus, GluK4 is absent. No other brain regions have high levels of GluK4 expression, although Purkinje neurons in the cerebellum express low amounts of mRNA and GluK4 protein (Darstein et al., 2003; Herb et al., 1992; Werner et al., 1991). The significance of this highly regionalized expression pattern of GluK4 is unclear but it is expected that heteromeric receptors containing GluK4 subunits will have distinct properties.

Kainate receptor function has been primarily examined in the hippocampus. The lack of selective pharmacological agents has remained an impediment to their study and has increased the importance of analyzing kainate receptor function in knockout mice (Contractor et al., 2003; Mulle et al., 1998; Mulle et al., 2000; Pinheiro et al., 2007). These studies demonstrated that kainate receptors are localized postsynaptically at some synapses, where they mediate a small component of the excitatory postsynaptic current ($EPSC_{KA}$) (Mulle et al., 1998). In addition, presynaptic kainate receptors bi-directionally modify synapse efficacy at both excitatory (Breustedt and Schmitz, 2004; Contractor et al., 2003; Contractor et al., 2000; Pinheiro et al., 2007) and inhibitory synapses (Mulle et al., 2000). Surprisingly, some of the actions of presynaptic kainate receptors are mediated by metabotropic signaling cascades divergent from their canonical function as ligand-gated cation channels (Frerking et al., 2001; Rodriguez-Moreno and Lerma, 1998). The metabotropic signaling of kainate receptors has also been demonstrated to have an altogether distinct action on cellular excitability through a long lasting inhibition of the slow Ca^{2+}-activated K^+ conductance (I_{sAHP}) (Melyan et al., 2004; Melyan et al., 2002).

NIH-PA Author Manuscript

NIH-PA Author Manuscript

NIH-PA Author Manuscript

The ionotropic and metabotropic actions of kainate receptors in hippocampal pyramidal neurons have been proposed to be differentially mediated by distinct component subunits, GluK2 and GluK5, respectively (Ruiz et al., 2005). It is unknown if the closely related high affinity subunit, GluK4, performs a similar function because pharmacological tools that discriminate between the different subunits have not been developed. To determine the contribution of high-affinity subunits in determining the properties of neuronal kainate receptors, we generated a GluK4 receptor subunit knockout mouse. Moreover, we eliminated both high-affinity subunits in a double knockout mouse by crossing GluK4 knockouts to a GluK5 knockout mouse (Contractor et al., 2003). Analysis of kainate receptor function in the hippocampus revealed that ablation of the GluK4 subunit led to a significant reduction in the synaptically-evoked kainate receptor EPSC ($EPSC_{KA}$) at mossy fiber synapses. In the double $GluK4^{-/-}/GluK5^{-/-}$ mice we did not observe any kainate mediated EPSCs at hippocampal mossy fiber synapses. GluK2 receptor protein expression was not significantly reduced, although there was a consistent reduction in synaptically localized receptors observed with immunoelectron microscopy. Despite equivalent surface expression of GluK2 in the hippocampus, agonist-evoked kainate receptor whole-cell currents were not observed in either CA1 or CA3 hippocampal neurons in the double knockout mice. In contrast to this loss of ionotropic function, low concentrations of kainate effectively inhibited the I_{sAHP} in CA3 pyramidal neurons from $GluK4^{-/-}$, $GluK5^{-/-}$, and $GluK4^{-/-}/GluK5^{-/-}$ mice. These studies demonstrate the surprising result that the high-affinity GluK4 and GluK5 subunits are essential for the normal ionotropic function of neuronal kainate receptors, but are not obligatory for linking kainate receptors to metabotropic signaling pathways.

Results

Presynaptic autoreceptor function in high-affinity kainate receptor knockout mice

In order to understand the function of the high-affinity kainate receptor subunits, GluK4 and GluK5 (formerly KA1 and KA2), we generated a mutant mouse in which we engineered loxP sites into intronic regions of the *Grik4* locus, flanking a crucial exon that encodes the M2 p-loop of the receptor channel (Supplementary figure S1A-C). Cre-mediated recombination of the two loxP sites resulted in deletion of this exon and loss of both the mRNA (figure S1D) and the protein product in $GluK4^{-/-}$ mice (figure S1E). These mice were crossed to the previously characterized GluK5 null mouse (Contractor et al., 2003) to produce a new strain with both high-affinity subunits deleted ($GluK4^{-/-}/GluK5^{-/-}$). There were no developmental (figure S1F) or behavioral phenotypes evident in these mice.

Neuronal kainate receptors have been best described in the hippocampus, where they have been functionally localized to both postsynaptic densities (Castillo et al., 1997; Mulle et al., 1998; Vignes and Collingridge, 1997) and presynaptic terminals and axons (Chittajallu et al., 1996; Contractor et al., 2000; Schmitz et al., 2000; Schmitz et al., 2001). Of the several different excitatory and inhibitory synapses where kainate receptors play a role in synaptic transmission, the mossy fiber synapse, formed between the axons of the dentate gyrus granule cells and the pyramidal neurons in the CA3 region, is a particularly good model for studying kainate receptor function. At this synapse, kainate receptors subserve both pre- and postsynaptic roles in modulating and mediating synaptic transmission and have been implicated in NMDA receptor-independent long-term potentiation (Bortolotto et al., 1999; Contractor et al., 2001). Both GluK4 and GluK5 are expressed in granule cells and CA3 pyramidal neurons, and are localized to the mossy fiber presynaptic boutons and postsynaptic density in CA3 pyramidal cell thorny excrescence spines (Darstein et al., 2003). At the mossy fiber synapse, two forms of presynaptic short-term plasticity, paired-pulse facilitation and frequency facilitation, are disrupted in mice in which either of the principal subunits GluK2 or GluK3 are ablated (Contractor et al.,

NIH-PA Author Manuscript

NIH-PA Author Manuscript

NIH-PA Author Manuscript

2001; Pinheiro et al., 2007). No such disruption in short term plasticity was observed in GluK5$^{-/-}$ mice (Contractor et al., 2003).

We first examined the contributions of GluK4 and GluK5 to presynaptic kainate receptor function at mossy fiber synapses in the knockout mice by recording from CA3 neurons in GluK4$^{-/-}$ mice and their wildtype (WT) littermates. Paired stimuli were given to evoke mossy fiber EPSCs and paired-pulse ratios measured at several interstimulus intervals. We found no difference in paired-pulse facilitation between GluK4$^{-/-}$ and WT mice at any of the interstimulus intervals (Figure 1Aiii; ns for all interstimulus intervals by 2-way ANOVA; n=14 for GluK4$^{-/-}$, n=11 for WT). Similarly, the facilitation of EPSC amplitudes observed when afferent stimulation frequency was increased from 0.05 Hz to 1 Hz was not different between recordings from GluK4$^{-/-}$ mutants and WT mice (379 ± 32%, n=13 for WT; 331 ± 43%, n=13 for GluK4$^{-/-}$; ns by 1-way ANOVA, Bonferroni post-test) (Figure 1Biii). Thus, elimination of GluK4 alone does not impact facilitation of transmission mediated by presynaptic kainate receptors, similar to what was found in GluK5 subunit knockout mice (Contractor et al., 2003).

To determine if elimination of both high affinity subunits had an impact on presynaptic autoreceptor function, we made similar recordings from GluK4/GluK5 double knockout mice (Figure 1A). In contrast to the single knockouts, we observed a significant difference in paired-pulse ratio measurements at the shortest interstimulus intervals from 20 - 100ms (WT at 20 ms: 3.26 ± 0.28; GluK4$^{-/-}$/GluK5$^{-/-}$ at 20ms: 2.44 ± 0.15; WT at 40 ms: 2.96 ± 0.26; GluK4$^{-/-}$/GluK5$^{-/-}$ at 40ms: 2.17 ± 0.07; WT at 100 ms: 2.69 ± 0.13; GluK4$^{-/-}$/GluK5$^{-/-}$ at 100ms: 2.27 ± 0.11; significant by 2-way ANOVA, WT, n=11; GluK4$^{-/-}$/GluK5$^{-/-}$, n=14). Prior studies in GluK2 (Contractor et al., 2001) and GluK3 (Pinheiro et al., 2007) knockout mice found that ablation of these primary subunits caused deficits in both paired-pulse facilitation and frequency facilitation. In contrast to this we found no parallel deficits in frequency facilitation in the GluK4$^{-/-}$/GluK5$^{-/-}$ mice (376 ± 41%, n=11 for GluK4$^{-/-}$/GluK5$^{-/-}$; ns from WT, 1-way ANOVA; Figure 1B). These results therefore differentiate at least two populations of presynaptic kainate receptors: (i) those containing GluK4 and/or GluK5 subunits positioned to respond to single release events (engaged during paired, high-frequency stimuli) and (ii) those receptors that mediate facilitation during longer, lower-frequency stimulations, possibly located further from the neurotransmitter release sites, which do not require GluK4 or GluK5 as component subunits.

The finding that paired-pulse facilitation is deficient in GluK4$^{-/-}$/GluK5$^{-/-}$ mice, while frequency facilitation is intact, raises an interesting dissociation of the involvement of kainate receptors in these two forms of plasticity. A recent study has questioned the importance of the contribution of presynaptic kainate receptors to mossy fiber synaptic facilitation (Kwon and Castillo, 2008). Therefore to determine if frequency facilitation in GluK4$^{-/-}$/GluK5$^{-/-}$ knockout mice was indeed, in part, mediated by a presynaptic autoreceptor, as has been repeatedly reported by other laboratories as well as our own (Breustedt and Schmitz, 2004; Contractor et al., 2001; Ji and Staubli, 2002; Kamiya et al., 2002; Lauri et al., 2001; Pinheiro et al., 2007; Schmitz et al., 2001; Scott et al., 2008), we performed further experiments using a pharmacological strategy to acutely antagonize kainate receptors. We recorded the mixed AMPA/NMDA EPSC and measured the NMDA receptor component 30 ms after the onset of the current (see Methods). In WT mice the NMDA component of the mossy fiber EPSC facilitated on average 260 ± 30 % (n=5) when the frequency of afferent stimulation was increased from 0.05Hz to 1Hz (Figure 1Ci). When the AMPA/kainate receptor antagonist CNQX (50 μM) was present the facilitation of the NMDA mossy fiber EPSC was significantly diminished ($p < 0.05$). In interleaved experiments in GluK4$^{-/-}$/GluK5$^{-/-}$ mice we observed a similar significant reduction in frequency facilitation of mossy fiber synaptic transmission by CNQX (Figure 1Cii). Therefore in both WT and GluK4$^{-/-}$/GluK5$^{-/-}$ mice it is clear that

NIH-PA Author Manuscript

NIH-PA Author Manuscript

NIH-PA Author Manuscript

facilitation of mossy fiber synaptic transmission is in part mediated by a facilitatory kainate autoreceptor.

Application of kainate receptor agonists has a biphasic effect on mossy fiber synaptic transmission; low concentrations enhance mossy fiber EPSCs whereas higher concentrations depress mossy fiber transmission (Schmitz et al., 2001). Both actions of kainate receptor ligands are abrogated in GluK2$^{-/-}$ (Breustedt and Schmitz, 2004; Contractor et al., 2000) but not GluK3$^{-/-}$ mice (Pinheiro et al., 2007). We previously found that low concentrations of kainate failed to facilitate the EPSC in GluK5$^{-/-}$ mice, but the depression by higher concentrations was intact (Contractor et al., 2003). To further refine our understanding of the contribution of individual subunits to modulation of mossy fiber synaptic transmission we determined whether biphasic kainate-mediated effects could be observed in GluK4$^{-/-}$/GluK5$^{-/-}$ mice. Application of 50 nM kainic acid significantly increased mossy fiber EPSCs in WT mice (120 ± 8.7 %, n=4, $p < 0.05$) whereas there was no significant change in the amplitude of the EPSC in recordings from GluK4$^{-/-}$/GluK5$^{-/-}$ mice (91 ± 4.8 %, n=5 $p > 0.05$) (Figure 1Di). Higher concentrations of kainic acid (500 nM) depressed the EPSC in both genotypes to the same degree (WT: 75 ± 6.5 %, n=5; GluK4$^{-/-}$/GluK5$^{-/-}$: 81 ± 5.8 %, n=7, $p > 0.05$) (Figure 1Dii).These agonist-induced effects on mossy fiber EPSCs are similar to what we previously reported in GluK5$^{-/-}$ mice (Contractor et al., 2003).

GluK4 and GluK5 are essential components of mossy fiber kainate receptor synaptic currents

Kainate receptors subserve a more traditional role in mediating postsynaptic ionotropic currents at some synapses, including the mossy fiber synapse (Castillo et al., 1997; Vignes and Collingridge, 1997). The mossy fiber kainate receptor-mediated EPSC ($EPSC_{KA}$) has slow kinetics that may be due in part to the slow deactivation conferred upon heteromeric receptors by the GluK5 subunit (Barberis et al., 2008). We previously reported that in GluK5$^{-/-}$ mice the mossy fiber $EPSC_{KA}$ decays significantly faster compared to the current decay in WT mice, whereas there is no observable alteration in the amplitude of the current (Contractor et al., 2003). To characterize how GluK4 subunits alter postsynaptic receptor function, we initially recorded mixed AMPA/kainate EPSCs from CA3 pyramidal neurons while stimulating mossy fiber afferents at 1 Hz to increase release probability. In WT mice, application of GYKI 53655 (100 μM) blocked the fast component of the EPSC, leaving a clearly measurable residual GYKI-resistant $EPSC_{KA}$ in all our recordings (Figure 2Ai & Aiii). In contrast, the slow $EPSC_{KA}$ was detected in only a subset of recordings from GluK4$^{-/-}$ mice (9 of 15 cells), and in those recordings the mean $EPSC_{KA}$ amplitude was lower than that observed in WT mice (Figure 2Aiii). The $EPSC_{KA}$ contributed only 2.3 ± 0.4% of the total AMPA/kainate peak current amplitude in GluK4$^{-/-}$ mice, approximately half that observed in WT recordings in which the amplitude of the $EPSC_{KA}$ was 4.9 ± 0.7 % of the total EPSC. Neurons from GluK4$^{-/-}$/GluK5$^{-/-}$ mice had an even more profound deficit in the $EPSC_{KA}$. In fact, in GluK4$^{-/-}$/GluK5$^{-/-}$ neurons we never detected a $EPSC_{KA}$ while stimulating mossy fiber afferents at 1 Hz as the mossy fiber EPSC was fully blocked by GYKI 53655 (n = 5) (Figure 2Aii & Aiii).

To examine $EPSC_{KA}$ in greater detail, we delivered short trains of high frequency stimulation at 100 Hz to increase release probability and maximize the postsynaptic mossy fiber response. In WT neurons train stimulation produced a large $EPSC_{KA}$ with a mean amplitude of 181 ± 46 pA (n=15). Fitting a single exponential component to the decay of this current gave a of 64 ± 7 ms, consistent with previous reports (Castillo et al., 1997; Contractor et al., 2003). In comparison, the amplitude of the train-induced $EPSC_{KA}$ was approximately half the WT amplitude in recordings from GluK4$^{-/-}$ mice (87 ± 12 pA, n=11; Figure 2Biv). In addition, the deactivation kinetics of this EPSC were significantly slower, with a mean τ of 127 ± 14 ms

NIH-PA Author Manuscript

NIH-PA Author Manuscript

NIH-PA Author Manuscript

(Figure 2Bv). This contrasts with the faster timecourse of decay of the $EPSC_{KA}$ and unaltered amplitude of kainate receptor-mediated EPSCs in GluK5$^{-/-}$ mice (Contractor et al., 2003).

Even more surprisingly, the high frequency train did not reveal the presence of any functional postsynaptic kainate receptors in recordings from GluK4$^{-/-}$/GluK5$^{-/-}$ mice; no $EPSC_{KA}$ remained after AMPA receptor inhibition in any of our recordings (n=8; Figure 2Biii). These data demonstrate that the GluK4 and GluK5 subunits are essential to the normal localization and/or function of postsynaptic kainate receptors in the hippocampus.

GluK2 subunits are trafficked to the plasma membrane in GluK4$^{-/-}$/GluK5$^{-/-}$ mice

GluK2 is the principal subunit expressed in CA3 pyramidal neurons, and we expected that this subunit would form functional homomeric receptors in the absence of GluK4 and GluK5. However, we were unable to detect any mossy fiber $EPSC_{KA}$ in the GluK4$^{-/-}$/GluK5$^{-/-}$ mice. Several possible explanations may underlie this observation: compromised GluK2 subunit expression, retention of homomeric GluK2 receptors in the endoplasmic reticulum (ER), or perhaps a failure to stabilize homomeric GluK2 at synaptic sites.

We performed several biochemical experiments to test these possibilities. First, we found that total GluK2/3 protein was not altered in the GluK4$^{-/-}$, GluK5$^{-/-}$ or GluK4$^{-/-}$/GluK5$^{-/-}$ mice relative to WT as determined by Western blot analysis of whole hippocampal membrane preparations, suggesting that there is not a large compensatory reduction in the expression of the primary subunits when the high-affinity subunits are ablated (Figure 3Ai & ii).

Second, we tested if GluK2 receptor subunits were sequestered in the ER in the absence of GluK4 and/or GluK5. Edited AMPA receptor subunits do not assemble efficiently (Greger et al., 2003) and it is possible that edited GluK2 receptor subunits could be similarly retained in the ER in GluK4$^{-/-}$/GluK5$^{-/-}$ mice. Glutamate receptors undergo glycolytic processing in the both ER and Golgi. Immature receptors in the ER can be distinguished from the receptors which have undergone further processing in the Golgi by treatment with endoglycosidase H (Endo H), which only digests immature oligosaccharides attached in the ER, and peptide: N-glycosidase F (PNGaseF) which cleaves all oligosaccharides. Therefore, an increased sensitivity to Endo H would indicate that a larger proportion of receptors were retained in the ER or that trafficking through the Golgi was slowed. We found that almost all the GluK2 protein was insensitive to Endo H digestion in WT mice, suggesting that under normal conditions GluK2 is efficiently exported from the ER and processed by Golgi-resident enzymes (Figure 3B). GluK2 subunit protein isolated from GluK4$^{-/-}$, GluK5$^{-/-}$ and GluK4$^{-/-}$/GluK5$^{-/-}$ mice showed similar resistance to Endo H digestion, effectively demonstrating that loss of synaptic currents is not accounted for by sequestration of the principal subunit GluK2 in the ER (Figure 3B).

Next, to determine if GluK2 subunit protein was detectable on the plasma membrane of neurons in the absence of the high affinity subunits, we performed surface biotinylation assays on hippocampal slices from WT and knockout mice (Thomas-Crusells et al., 2003). Acute brain slices were exposed to the sulfo-NHS-LC-biotin labeling reagent, or control solution, before processing and isolation of membrane proteins using streptavidin-sepharose beads. Western blots with anti-GluK2/3 antibody were performed after separation on SDS-PAGE. We detected no significant alteration in the surface expression of GluK2/3 in hippocampal slices in any of the mouse genotypes tested, with the exception of slices from GluK2$^{-/-}$ knockout mice used as a negative control in this assay (Figure 3C). We also probed membranes with antibodies against the intracellular protein β-tubulin as a control for selective isolation of plasma membrane receptor subunits. As expected, β-tubulin was absent from the biotinylated fraction but present in abundance in the non-biotinylated (total membrane lysate) samples (not shown). Taken together, these results indicate that there are no gross alterations in total expression or

NIH-PA Author Manuscript

NIH-PA Author Manuscript

NIH-PA Author Manuscript

surface localization of GluK2/3 in the hippocampus in mice lacking the GluK4 and GluK5 subunits.

Subcellular distribution of kainate receptors is altered in GluK4$^{-/-}$/GluK5$^{-/-}$ mice

The preceding series of experiments suggested that the loss of synaptic kainate receptor function cannot be fully ascribed to a loss of plasma membrane expression of GluK2 in GluK4$^{-/-}$/GluK5$^{-/-}$ mice. In order to assess whether we could detect more subtle changes in kainate receptor localization, we performed immunogold electron microscopy on CA3 mossy fiber synapses. Hippocampal sections were taken from three WT and three GluK4$^{-/-}$/GluK5$^{-/-}$ mice and labeled with α-GluK2/3 antibody. Gold particles were quantified in sections containing the large mossy fiber boutons (MFB) and postsynaptic thorny excrescence spines (SP) (WT:173 spine profiles; knockout: 215 spine profiles) (Figure 4). We observed many fewer GluK2/3-immunoreactive gold particles associated with the spine membrane in GluK4$^{-/-}$/GluK5$^{-/-}$ sections relative to WT (Total spine) (Figure 4C), whereas cytoplasmic-localized gold particles were reduced only marginally in knockouts, resulting in a decrease in the total spine membrane to cytoplasm ratio in the knockout mice (Figure 4C). Quantification of gold particles in postsynaptic spines (blue arrows in Figure 4A & 4B) revealed profound reductions in the number of gold particles both in the postsynaptic density (PSD) and in the peri-synaptic region of GluK4$^{-/-}$/GluK5$^{-/-}$ sections. Similarly, GluK2/3-immunoreactivity was present at significantly lower levels at active zones and peri-synaptic domains of presynaptic MFBs (Figure 4E). These results match well with physiological data and demonstrate that effective localization of kainate receptors containing the GluK2 subunits to pre- and postsynaptic sites requires the GluK4 and GluK5 subunits.

Activation of extrasynaptic kainate receptors

Our EM analysis demonstrated that GluK2 receptors appeared to be distributed away from mossy fiber synaptic sites in the absence of GluK4 and GluK5. However, extrasynaptic plasma membrane kainate receptors appear to be abundant in these mice as evidenced by the equivalent levels of biotinylated, surface GluK2/3 protein in knockout and WT hippocampi (Figure 3C). We next tested if those extra-synaptic receptors were functional by bath-applying agonists during whole-cell patch clamp recordings from CA3 pyramidal neurons. The exogenous agonist kainate (10 μM) was applied in the presence of antagonists of AMPA (100 μM GYKI 53655), NMDA (50 μM D-APV) and $GABA_A$ (10 μM bicuculline and 50 μM picrotoxin) receptors. In WT mice, this concentration of kainate elicited a large amplitude inward current in all recordings, with a mean of 1050 ± 252 pA (n=13)(Figure 5Ai). In GluK4$^{-/-}$ mice, however, the mean current amplitude elicited by kainate was significantly smaller (213 ± 26, n=10, $p < 0.01$)(Figure 5Aii). Surprisingly, no change in membrane current was associated with kainate application to CA3 neurons in slices from GluK4$^{-/-}$/GluK5$^{-/-}$ mice (n=9) (Figure 5Aiii & B). This was not a CA3-specific phenomenon, because 10 μM kainate also failed to elicit a current from CA1 pyramidal neurons from GluK4$^{-/-}$/GluK5$^{-/-}$ mice (n=5), whereas in WT CA1 neurons a small inward current was observed in all neurons tested (90 ± 49 pA, n=3).

The absence of whole-cell currents in GluK4$^{-/-}$/GluK5$^{-/-}$ neurons could arise from a profound desensitization of the receptors by kainate relative to receptors in WT neurons, rather than reflecting a difference in the number of channels. To maximize our ability to detect putative homomeric GluK2 receptors electrophysiologically, we instead applied domoate (10 μM), a high-affinity agonist that desensitizes recombinant GluK2 receptors to a lesser degree and evokes relatively large steady-state currents (Swanson et al., 1997). We again observed large currents in WT CA3 pyramidal neurons that were similar in mean amplitude to those evoked by 10 μM kainate (1350 ± 191 pA, n=5). In recordings from GluK4$^{-/-}$/GluK5$^{-/-}$ neurons, domoate reliably induced currents in all our recordings, although these were of significantly

NIH-PA Author Manuscript

NIH-PA Author Manuscript

NIH-PA Author Manuscript

lower mean amplitude (165 ± 16 pA, n=6, $p < 0.01$) (Figure 5C). Therefore GluK2 receptors are functional in the absence of GluK4 and GluK5, but it seems likely that both a change in biophysical function and membrane localization (perhaps too subtle to be detected in the biotinylation assay) contribute to the extreme attenuation of ionotropic responses observed in double knockout mice. Taken together, these data demonstrate that native kainate receptors do not function efficiently as ion channels when GluK4 and GluK5 are not available to form heteromeric receptor assemblies.

Metabotropic signaling by kainate receptor is intact in GluK4$^{-/-}$/GluK5$^{-/-}$ mice

In addition to their classic activity as receptor-ion channels, there is increasing evidence that kainate receptors signal through metabotropic pathways to execute aspects of their presynaptic regulatory activity as well as a postsynaptic function as inhibitors of intrinsic conductances that control cellular excitability (Rodriguez-Moreno and Sihra, 2007). In particular it has been demonstrated that the post-burst slow afterhyperpolarization (I_{sAHP}), a conductance generated by a Ca^{2+}-activated K^+ current, is inhibited by kainate receptors through a metabotropic signaling pathway (Melyan et al., 2004; Melyan et al., 2002). Deletion of GluK2 eliminated this regulation in hippocampal CA3 neurons (Fisahn et al., 2005), although it was also proposed recently that GluK5 subunits were critical for metabotropic signaling, because this modulatory activity was lost in GluK5$^{-/-}$ mice (Ruiz et al., 2005). In order to determine if GluK4 might be required for this role of kainate receptors, we made voltage clamp recordings from CA3 neurons and activated the I_{sAHP} current with a brief depolarization of the neuron (50 mV for 80 ms). I_{sAHP} was monitored every 30s; after a stable five minute baseline period, a low concentration of kainate (50 nM) was applied. In WT recordings, the I_{sAHP} was depressed by 33 ± 4 % in the presence of kainate (n=8) (Figure 6A & C). Surprisingly, I_{sAHP} was inhibited by kainate to the same degree in both GluK4$^{-/-}$ (25 ± 8 %, n=4) and GluK5$^{-/-}$ mice (36 ± 9 %, n=4), (contrary to prior published results (Ruiz et al., 2005)), which we included in the experimental design as a "positive" control for loss of the inhibitory action (Figure 6C). Metabotropic signaling was similarly unaffected in GluK4$^{-/-}$/GluK5$^{-/-}$ mice; 50nM kainate depressed the I_{sAHP} in CA3 pyramidal neurons by 27 ± 3 % (n=7, $p > 0.05$) (Figure 6B & C). To further confirm these results we looked at kainate receptor inhibition of I_{sAHP} using a broader range of kainic acid concentration ranging from 20nM to 500nM. In these recordings we also saw that I_{sAHP} inhibition in GluK4$^{-/-}$/GluK5$^{-/-}$ mice was not different to that observed in WT recordings (Figure 6D). These results demonstrate that in CA3 pyramidal neurons, kainate receptors retain their ability to link to metabotropic signaling pathways to depress the I_{sAHP} in the absence of the high affinity subunits and detectable ionotropic function.

Discussion

High affinity subunits are critical constituents for ionotropic kainate receptor function

Kainate receptors are atypical members of the glutamate receptor family because they seem to have diverse physiological roles and signaling modalities which are determined primarily by their subunit composition and subcellular distribution to a variety of compartments within neurons (Pinheiro and Mulle, 2006). Generation of a complete set of kainate receptor knockout mice has greatly facilitated our understanding of the spectrum of neuronal functions subserved by kainate receptors, and most particularly those receptors with component subunits whose activity cannot be manipulated with existing pharmacological tools. Here we used a newly generated GluK4$^{-/-}$ mouse, together with a GluK4$^{-/-}$/GluK5$^{-/-}$ mouse, to determine the specific contribution of the high-affinity subunits to neuronal kainate receptor function. Our most surprising finding was that loss of both GluK4 and GluK5 led to a complete loss of detectable $EPSC_{KA}$ at mossy fiber synapses. This was unexpected in part because the principal subunit GluK2, which is capable of forming functional homomeric receptors, was expressed at normal levels and was abundantly localized to plasma membranes in the hippocampus of

NIH-PA Author Manuscript

NIH-PA Author Manuscript

NIH-PA Author Manuscript

GluK4$^{-/-}$/GluK5$^{-/-}$ mice. This profound deficit was not apparent in recordings from the single GluK4$^{-/-}$ or GluK5$^{-/-}$ knockouts (Contractor et al., 2003), in which mossy fiber EPSCs$_{KA}$ were readily detected, albeit with clear alterations in biophysical function and, in the case of GluK4, markedly attenuated current amplitudes. These results demonstrate the critical importance of the high affinity subunits to synaptic kainate receptor function.

In addition to an apparent functional deficit in the GluK4$^{-/-}$/GluK5$^{-/-}$ mice, a redistribution of GluK2-containing kainate receptors away from mossy fiber synapses likely contributes to the loss of EPSC$_{KA}$. We observed clear reductions in the total number of labeled particles associated with the membranes of mossy fiber thorny excrescences and an decreased ratio of membrane to cytoplasmic particles in GluK4$^{-/-}$/GluK5$^{-/-}$ mice. Therefore, localization of the principal kainate receptor subunits GluK2 and GluK3 are dependent on incorporation of the high affinity subunits into a heteromeric receptor complex. The immuno-EM data matches well with the physiological evidence for alterations in pre- and postsynaptic mossy fiber function. That is, the absence of a postsynaptic ionotropic response in the double knockout mice, even during high-frequency trains, correlates with an approximately 75% loss of postsynaptic PSD labeling and a >50% loss of peri-synaptic labeling.

Presynaptic labeling of GluK2-containing receptors is also reduced in the absence of the high affinity subunits, but the alteration in function is more subtle than occurs with genetic ablation of either GluK2 and GluK3, the principal subunit constituents of presynaptic autoreceptors at the mossy fiber synapse (Contractor et al., 2001; Pinheiro et al., 2007). GluK2 and GluK3 knockout mice exhibit deficits in two forms of short term facilitation, induced either by pairing stimuli (paired-pulse facilitation) or using sustained elevated frequency stimulation (frequency facilitation) (Breustedt and Schmitz, 2004; Contractor et al., 2001; Pinheiro et al., 2007). In the current study, our analysis using immuno-EM revealed an almost complete loss of labeled particles associated with the presynaptic active zone and a reduction to a lesser extent of peri-synaptic particles in mossy fiber boutons. In physiological studies, we found that paired stimuli facilitated mossy fiber EPSCs to a lesser degree in GluK4$^{-/-}$/GluK5$^{-/-}$ mice relative to WT mice, while low-frequency facilitation remained unaltered. This dissociation between two forms of short term facilitation raised the question whether the intact frequency facilitation in GluK4$^{-/-}$/GluK5$^{-/-}$ mice was in fact mediated by kainate receptors. We therefore performed a further experiment in which we acutely blocked kainate receptors with a competitive antagonist. In both WT and GluK4$^{-/-}$/GluK5$^{-/-}$ mice, CNQX significantly inhibited facilitation of the NMDA component of the mossy fiber EPSC, confirming a role for kainate receptors in this form of short term plasticity. Based on these data, we propose that high affinity subunits effectively localize presynaptic kainate receptors near release sites, positioning the receptors to respond to synaptic glutamate released during sparse presynaptic activity. Genetic ablation of the GluK4 and GluK5 subunits destabilizes presynaptic kainate receptor localization near release sites, distributing the receptor to more remote sites where they remain able to respond to sustained glutamate transients evoked by longer trains of stimuli.

These data provide additional support for a role of presynaptic kainate receptors in facilitating mossy fiber excitatory transmission, which was recently called into question (Kwon and Castillo, 2008). Kwon and Castillo proposed that facilitation of mixed AMPA/kainate EPSCs apparently mediated by presynaptic kainate receptors could be accounted for instead by postsynaptic kainate receptor-driven excitation of neighboring CA3 pyramidal neurons during mossy fiber stimulation, leading to rapid polysynaptic input to the neuron under voltage clamp, and over-estimation of “true” facilitation arising from presynaptic mechanisms. Our data from the GluK4$^{-/-}$/GluK5$^{-/-}$ mice are inconsistent with this hypothesis. That is, frequency facilitation during 1 Hz stimulation was equivalent in WT and double knockout mice - despite the absence of a postsynaptic kainate receptor current in CA3 neurons from knockout animals. Postsynaptic kainate receptors therefore do not underlie frequency facilitation of mossy fiber

NIH-PA Author Manuscript

NIH-PA Author Manuscript

NIH-PA Author Manuscript

transmission. The specific reduction in paired-pulse ratios, but not low-frequency facilitation of excitatory transmission, in the double knockout animals further support the existence of discrete populations of presynaptic kainate receptors responsive to differing glutamate concentration profiles. Finally, we note that the marked increase in polysynaptic input postulated by Kwon and Castillo was not observed in either our current or previous recordings of mossy fiber EPSCs; indeed, the preponderance of biochemical and physiological evidence supports a key role for facilitatory kainate receptors at mossy fiber synapses (Contractor et al., 2001; Darstein et al., 2003; Lauri et al., 2001; Pinheiro and Mulle, 2008; Pinheiro et al., 2007; Schmitz et al., 2001; Scott et al., 2008).

Role of the high affinity subunits in modulation of I_{sAHP}

One of the more intriguing aspects of kainate receptor function is that activation of these receptors leads to bimodal signaling through both ionotropic and metabotropic mechanisms. Metabotropic kainate receptors appear to engage G proteins, PKC and PKA to inhibit I_{sAHP} (Grabauskas et al., 2007; Melyan et al., 2004; Melyan et al., 2002; Rodriguez-Moreno and Sihra, 2007), a voltage independent, Ca^{2+}-dependent potassium conductance activated for several seconds following a burst of action potentials, which limits further firing and contributes to spike frequency adaptation. This inhibition is irreversible and might in large part account for the long lasting excitability caused by kainate receptor activation in the CNS (Westbrook and Lothman, 1983). Kainate-mediated inhibition of I_{sAHP} is absent from GluK2 knockout animals, which do not express functional kainate receptors in CA3 pyramidal neurons, clearly demonstrating that kainate receptors underlie this modulation (Fisahn et al., 2005). More recently, Ruiz and colleagues reported the provocative observation that metabotropic inhibition of I_{sAHP} in GluK5$^{-/-}$ mice was absent (Ruiz et al., 2005), even though the ionotropic function of kainate receptors is only modestly affected by loss of this subunit (Contractor et al., 2003). Surprisingly, we were unable to reproduce this result, finding instead that I_{sAHP} inhibition in CA3 pyramidal neurons was completely intact in GluK5$^{-/-}$ mice, as well as GluK4$^{-/-}$ and GluK4$^{-/-}$/GluK5$^{-/-}$ mice over a range of kainic acid concentrations. The reasons for these discrepancies remain unresolved but are not accounted for by strain differences between our animals and those used by Ruiz and colleagues (mice originated from the same source), or by large differences in experimental details, as we used similar recording conditions. Nevertheless, our data provide further support for the hypothesis that metabotropic mechanisms underlie this modulatory activity, because inhibition of I_{sAHP} occurred in the absence of agonist-evoked channel currents. Therefore, based on the current study we are compelled to conclude that the high affinity subunits GluK4 and GluK5 are not necessary for metabotropic signaling of kainate receptors.

In conclusion, the generation of GluK4$^{-/-}$ knockout mice enabled us to identify the important role played by the high affinity subunits in neuronal kainate receptor function and localization at synapses in the hippocampus. We find that localization of kainate receptors near the postsynaptic density and on presynaptic membranes near active zones is critically dependent on the GluK4 and GluK5 subunits. Moreover, without the high affinity subunits, both synaptic and extrasynaptic kainate receptors do not function efficiently as ligand-gated ion channels but remain capable of activating metabotropic pathways to modulate neuronal excitability.

Methods

Generation of GluK4 knockout mice

A targeting construct was generated containing two lox P sites flanking exon 14 of the *Grik4* gene and 5′ and 3′ arms with positive and negative selection markers (see figure S1). Standard techniques were used to target embryonic mouse cells and following homologous recombination positive clones were injected into blastocysts and transferred to pseudo pregnant

NIH-PA Author Manuscript

NIH-PA Author Manuscript

NIH-PA Author Manuscript

females. Germ-line transmission was determined by chimeric animals and genotyping of founders by PCR. Global knockout of *Grik4* was achieved by crossing with a transgenic mouse expressing Cre recombinase under the protamine 1 promoter (O'Gorman et al., 1997). Expression of Cre recombinase is found in the male sperm of these mice and leads to recombination of loxP sites in all tissues (Xu et al., 2009). Animals were backcrossed to a 129Sv strain and subsequently crossed with GluK5$^{-/-}$ animals to create a double GluK4$^{-/-}$/GluK5$^{-/-}$ knockout.

Slice preparation and electrophysiological recordings—For electrophysiological recordings transverse horizontal hippocampal slices (350 μm) from the ventral region of the hippocampus were prepared from juvenile mice P14-28. Animals were anesthetized with isoflurane and decapitated. The brain was rapidly removed under ice-cold oxygenated sucrose-slicing ACSF containing: 85 mM NaCl, 2.5 mM KCl, 1.25 mM NaH_2PO_4, 25 mM $NaHCO_3$, 25 mM glucose, 75 mM sucrose, 0.5 mM $CaCl_2$, and 4 mM $MgCl_2$, equilibrated with 95% O_2/5% CO_2. Slices were incubated at 28°C for 30 minutes, and a slow exchange was made of the oxygenated sucrose-ACSF for oxygenated sodium-ACSF solution containing: 125 mM NaCl, 2.4 mM KCl, 1.2 mM NaH_2PO_4, 25 mM $NaHCO_3$, 25 mM glucose, 1 mM $CaCl_2$, and 2 mM $MgCl_2$. Tail biopsies were taken from all mice used in experiments in order to determine genotype. Individual slices were transferred to a recording chamber and visualized under Normarski optics. Slices were continuously perfused with oxygenated sodium ACSF containing 2 mM $CaCl_2$ and 1 mM $MgCl_2$. All recordings were performed at elevated temperature (30°C). Whole-cell voltage clamp recordings were made from visually identified neurons using a Multiclamp 700B patch clamp amplifier (Axon Instruments). Glass electrodes were pulled from borosilicate glass and had resistances of 3-4 MΩ when filled with internal solution. For whole-cell voltage clamp recordings a CsF internal solution was used containing: 95mM CsF, 25mM CsCl, 10mM Cs-HEPES, 10mM Cs-EGTA, 2mM NaCl, 2mM Mg-ATP, 10mM QX-314, 5mM TEA-Cl, 5mM 4-AP, pH adjusted to 7.3 with CsOH. For voltage clamp recordings of I_{sAHP} the internal solution contained: 125 mM $KMeSO_4$, 5 mM KCl, 5 mM NaCl, 0.02mM EGTA, 11mM HEPES, 1 mM MgCl, 10mM phosphocreatine, 4 mM Mg-ATP, 0.3 mM Na-GTP. Series resistance was continuously monitored using hyperpolarizing voltage steps generated by pClamp 9 software (Axon Instruments), and recordings were discarded if there was a >15% change during the course of the experiment. For mossy fiber synaptic experiments EPSCs were isolated using the $GABA_A$ antagonists bicuculline (10 μM) and picrotoxin (100 μM), and the NMDA receptor antagonist, D-APV (50 μM). Mossy fiber synaptic currents were evoked by a monopolar glass electrode filled with oxygenated ACSF positioned in the stratum lucidum (Armstrong et al., 2006; Contractor et al., 2002; Contractor et al., 2003). For frequency facilitation recordings of the NMDA component, the mossy fiber EPSC was recorded (in the absence of D-APV and presence of saturating glycine, 10 μM) while briefly depolarizing the CA3 neuron (+40mV). The NMDA component was measured as the amplitude mean during a 2.5ms window 30ms after the onset of the current. At this time-point we determined that the AMPA component of the EPSC had completely decayed, while the postsynaptic kainate receptor mediated component was negligible.

Stimuli were controlled by pClamp 9 software and generated with an A310 Accupulser coupled to an A360 stimulation isolation unit. Data collection and analysis were performed with pClamp 9, Microsoft Excel and Microcal Origin software. Two sample comparisons were made using the paired Student's t-test and multiple comparisons were made using a one-way analysis of variance (ANOVA). The n represents number of individual recordings. Only one recording was made from each slice and at least three animals were used for each experiment. Mossy fiber EPSCs were identified by large paired pulse facilitation, brief onset latencies and rapid EPSC rise-times, and by the addition of the group II mGluR agonist DCG-IV (1 μM) (Armstrong et al., 2006).

NIH-PA Author Manuscript

NIH-PA Author Manuscript

NIH-PA Author Manuscript

Protein blots—Mice were anesthetized with isoflurane and decapitated. Brains were dissected out, and hippocampi were removed. The tissue samples were rapidly frozen on dry ice and homogenized in 1 ml of lysis buffer (50 mM Tris, pH 7.5; 150 mM NaCl; 1 mM EDTA; 1% Triton X-100; 1% SDS; Complete Mini protease inhibitor cocktail tablets (Roche Diagnostics), followed by centrifugation for 5 min at 10,000 RCF to remove the insoluble fraction. The protein concentrations in each sample were calculated using a BCA Protein Assay Kit (Pierce Chemical). Samples containing 15 μg of protein were dissolved in a reducing sample buffer (Fisher Scientific), sonicated for 1 min, and boiled for 5 min. Samples were then separated via SDS-PAGE on a 10% polyacrylamide gel and transferred to a PVDF membrane (Pall Corporation). Membranes were blocked with 5% powdered milk in Tris-buffered saline/Tween-20 (TBS-T) and incubated with antibodies against GluR6/7 (1:1000, Chemicon), or β-actin (1:20,000, Sigma) overnight at 4 °C. Membranes were washed in TBS-T, and then probed with horseradish peroxidase-conjugated antibodies against either rabbit IgG or mouse IgG (1:50,000, Jackson ImmunoResearch) for one hour at room temperature. Following a final wash in TBS-T, membranes were incubated with LumiLight Western Blotting Substrate (Roche), after which they were allowed to expose X-ray film. Images were analyzed with ImageJ software. Each experiment was repeated in triplicate with tissue from at least three animals of each genotype in each experiment.

RT-PCR—Mouse hippocampi were dissected, rapidly frozen, and homogenized in TRIzol reagent (Invitrogen). Total RNA was extracted and 10 μg of the RNA was treated with DNase I (Promega) for 30 min at 37 °C. cDNA was synthesized by treating 2.5 μg of the DNase-treated RNA with avian myeloblastosis virus reverse transcriptase and random hexamer primers (Promega) for 1 h at 37 °C. PCR was performed on the cDNA to amplify a region spanning that encoded for by the targeted exon in GluK4 using the following primers: 5′-ATCCCTTTTCTCCAGGAGTC -3′ and 5′- CAGGTCATCCACAGACTCAA -3′. As a positive control for the RT reaction, cDNA was also subjected to PCR amplification of a region corresponding to GluK2 with the following primers: 5′- TTCGACTTAAAATTCGTCAGC -3′ and 5′- CATATGGTTCTTCCAAAATGG -3′. PCR products were electrophoresed, stained with ethidium bromide, and visualized with a UV transilluminator.

EndoH/PNGaseF Assay—Mice (P15-21) were anesthetized with isoflurane and decapitated. The hippocampus was removed from the cortex in ice-cold Tris buffer (10 mM, pH=7.4). Following dissection, the tissue was homogenized in cold lysis buffer (10 mM Tris, 50 mM NaCl, 1% Triton X-100, and protease inhibitor cocktail (P2714; Sigma) consisting of 1 mM 4-(2-aminoethyl)-benzenesulfonylfluoride-HCl, 0.8 μM aprotinin, 20 μM leupeptin, 40 μM bestatin, 15 μM pepstatin A, and 14 μM L-*trans*-epoxysuccinyl-leucylamido(4-guanidino) butane; pH = 7.6). Lysates were rotated for 1 hour at 4°C to solubilize proteins. Lysates were cleared by centrifugation at 12,000g for 30 minutes at 4°C, and the protein concentration of the supernatant was determined.

10 μg of protein was heated at 95°C for 10 minutes in the presence of glycoprotein denaturing buffer (P0702; New England Biolabs (NEB)). Following denaturation, G5 glycosidase buffer (NEB) was added to the undigested and EndoH samples, while G7 glycosidase buffer (NEB) and 1% NP-40 were added to the PNGaseF samples. 500 units of EndoH (P0702; NEB) were used to remove high-mannose containing oligosaccharides while an equal amount of PNGaseF (P0704; NEB) was used to remove all *N*-linked oligosaccharides. All samples were digested at 37°C for 1 hour. Reactions were stopped by addition of 2× Laemmli buffer (Bio-Rad) containing β-mercaptoethanol and heated at 95°C for 5 minutes. Samples were then separated by SDS-PAGE and electrotransferred onto polyvinylidene difluoride membranes (Millipore). Membranes were probed with rabbit anti-GluR6/7 antibody (1 μg/mL; AB5683; Millipore) overnight at 4°C. Immunoreactive bands were visualized using HRP-conjugated anti-rabbit secondary antibody (1:5000; NA934V, Amersham) for 1 hour at room temperature. Bands

NIH-PA Author Manuscript

NIH-PA Author Manuscript

NIH-PA Author Manuscript

were visualized using West Pico chemiluminescent substrate (34080; Pierce Biotech), followed by Hyperfilm ECL exposure (28-9068-35; Amersham).

Surface Biotinylation of slices—Hippocampal slices were prepared as described for electrophysiology. After 1 hour, slices were transferred into 6-well plates containing 0.5 mg/mL sulfo-NHS-LC-Biotin (21335; Pierce). Slices were biotinylated for 30 minutes on ice, followed by two washes with 50 mM NH_4Cl in ACSF and then two final washes in ACSF. The hippocampus was then dissected from each slice and homogenized in 1 mL homogenization buffer (10 mM Tris, 320 mM sucrose, protease inhibitors; pH=7.4). Samples were then cleared by centrifugation at 1000 xg for 5 minutes. The supernatants were collected and then centrifuged for 1 hour at 100,000 xg. The pellet was then resuspended in 500 μL lysis buffer (20 mM HEPES, 150 mM NaCl, 2 mM EDTA, 1% Triton X-100, 0.1% SDS, protease inhibitors; pH=7.4). Samples were sonicated and rotated for 1 hour at 4°C to solubilize proteins. The samples were then centrifuged for 40 minutes at 100,000 xg and the protein concentration of the supernatant was determined. 300 μg protein (300 μL final volume) from each mouse was then incubated with 40 μL of washed streptavidinsepharose beads (17-5113-01; Amersham) overnight at 4°C. Samples were centrifuged at 3000 rpm for 3 minutes and the supernatant was collected (non-biotinylated). Beads were then washed 3 times with lysis buffer and protein was eluted by heating at 95°C for 5 minutes with 150 μL 2× Laemmli sample buffer (Bio-Rad) containing β-mercaptoethanol. 40 μL from each sample was separated by SDS-PAGE and immunoblotted. Blots were stripped and re-probed with rabbit anti-β-tubulin III (1:10,000; T2200; Sigma) to ensure that intracellular protein was not biotinylated. Blots were stripped a final time and re-probed with avidin-HRP (N100; Pierce) to ensure that all biotinylated protein was pulled-down by the streptavidin beads.

Immunogold electron microscopy—Detailed methods for postembedding immunogold labeling have been described elsewhere (Petralia and Wenthold, 1999). Briefly, mice were perfused with 4% paraformaldehyde plus 0.5% glutaraldehyde and sections were frozen in liquid propane in a Leica CPC and freeze-substituted into Lowicryl HM-20 in a Leica AFS. Ultrathin sections were incubated in 0.1% sodium borohydride plus 50 mM glycine in Tris-buffered saline plus 0.1% Triton X-100 (TBST), and then in 10% normal goat serum (NGS) in TBST, and then primary antibody in 1% NGS/TBST, followed by 10 nm immunogold [F(ab')2 goat anti-rabbit, Ted Pella] in 1% NGS/TBST/0.5% polyethylene glycol (MW 20,000), and stained with uranyl acetate and lead citrate, and examined in a JEOL JEM-1010 electron microscope. A random sample of synapses was photographed and counted from 3 WT (173 spine profiles) and 3 $GluK4^{-/-}/GluK5^{-/-}$ mice (215 spine profiles). For this study, gold counts in the “peri-synaptic region” included the membrane of the thorny excrescence spine profile excluding the PSDs, or the region of the mossy terminal membrane apposed to the spine profile excluding the active zones.

Supplementary Material

Refer to Web version on PubMed Central for supplementary material.

Acknowledgments

We gratefully thank Professor Stephen Heinemann in whose laboratory the floxed GluK4 mice were originally generated. Ashley Westwood provided technical help with mouse husbandry and genotyping and Dr Ya-Xian Wang contributed to the immunogold labeling. This work was supported by extramural grants from the National Institute of Health (NINDS) (R01NS044322 to GTS & R01NS058894 to AC) and NIH intramural support (NIDCD) (to RSP). Justin Catches is a John N. Nicholson Fellow.

NIH-PA Author Manuscript

NIH-PA Author Manuscript

NIH-PA Author Manuscript

References

Armstrong JN, Saganich MJ, Xu NJ, Henkemeyer M, Heinemann SF, Contractor A. B-ephrin reverse signaling is required for NMDA-independent long-term potentiation of mossy fibers in the hippocampus. J Neurosci 2006;26:3474–3481. [PubMed: 16571754]

Bahn S, Volk B, Wisden W. Kainate receptor gene expression in the developing rat brain. J Neurosci 1994;14:5525–5547. [PubMed: 8083752]

Barberis A, Sachidhanandam S, Mulle C. GluR6/KA2 kainate receptors mediate slow-deactivating currents. J Neurosci 2008;28:6402–6406. [PubMed: 18562611]

Bortolotto ZA, Clarke VR, Delany CM, Parry MC, Smolders I, Vignes M, Ho KH, Miu P, Brinton BT, Fantaske R, et al. Kainate receptors are involved in synaptic plasticity. Nature 1999;402:297–301. [PubMed: 10580501]

Breustedt J, Schmitz D. Assessing the role of GluK5 and GluK6 at hippocampal mossy fiber synapses. J Neurosci 2004;24:10093–10098. [PubMed: 15537878]

Castillo PE, Malenka RC, Nicoll RA. Kainate receptors mediate a slow postsynaptic current in hippocampal CA3 neurons. Nature 1997;388:182–186. [PubMed: 9217159]

Chittajallu R, Vignes M, Dev KK, Barnes JM, Collingridge GL, Henley JM. Regulation of glutamate release by presynaptic kainate receptors in the hippocampus. Nature 1996;379:78–81. [PubMed: 8538745]

Contractor A, Rogers C, Maron C, Henkemeyer M, Swanson GT, Heinemann SF. Trans-synaptic Eph receptor-ephrin signaling in hippocampal mossy fiber LTP. Science 2002;296:1864–1869. [PubMed: 12052960]

Contractor A, Sailer AW, Darstein M, Maron C, Xu J, Swanson GT, Heinemann SF. Loss of kainate receptor-mediated heterosynaptic facilitation of mossy-fiber synapses in $KA2^{-/-}$ mice. J Neurosci 2003;23:422–429. [PubMed: 12533602]

Contractor A, Swanson G, Heinemann SF. Kainate receptors are involved in short- and long-term plasticity at mossy fiber synapses in the hippocampus. Neuron 2001;29:209–216. [PubMed: 11182092]

Contractor A, Swanson GT, Sailer A, O'Gorman S, Heinemann SF. Identification of the kainate receptor subunits underlying modulation of excitatory synaptic transmission in the CA3 region of the hippocampus. J Neurosci 2000;20:8269–8278. [PubMed: 11069933]

Darstein M, Petralia RS, Swanson GT, Wenthold RJ, Heinemann SF. Distribution of kainate receptor subunits at hippocampal mossy fiber synapses. J Neurosci 2003;23:8013–8019. [PubMed: 12954862]

Fisahn A, Heinemann SF, McBain CJ. The kainate receptor subunit GluR6 mediates metabotropic regulation of the slow and medium AHP currents in mouse hippocampal neurones. J Physiol 2005;562:199–203. [PubMed: 15539395]

Frerking M, Schmitz D, Zhou Q, Johansen J, Nicoll RA. Kainate receptors depress excitatory synaptic transmission at CA3-->CA1 synapses in the hippocampus via a direct presynaptic action. J Neurosci 2001;21:2958–2966. [PubMed: 11312279]

Grabauskas G, Lancaster B, O'Connor V, Wheal HV. Protein kinase signalling requirements for metabotropic action of kainate receptors in rat CA1 pyramidal neurones. J Physiol 2007;579:363–373. [PubMed: 17158174]

Greger IH, Khatri L, Kong X, Ziff EB. AMPA receptor tetramerization is mediated by Q/R editing. Neuron 2003;40:763–774. [PubMed: 14622580]

Herb A, Burnashev N, Werner P, Sakmann B, Wisden W, Seeburg PH. The KA-2 subunit of excitatory amino acid receptors shows widespread expression in brain and forms ion channels with distantly related subunits. Neuron 1992;8:775–785. [PubMed: 1373632]

Ji Z, Staubli U. Presynaptic kainate receptors play different physiological roles in mossy fiber and associational-commissural synapses in CA3 of hippocampus from adult rats. Neurosci Lett 2002;331:71–74. [PubMed: 12361843]

Kamiya H, Ozawa S, Manabe T. Kainate receptor-dependent short-term plasticity of presynaptic Ca^{2+} influx at the hippocampal mossy fiber synapses. J Neurosci 2002;22:9237–9243. [PubMed: 12417649]

NIH-PA Author Manuscript

NIH-PA Author Manuscript

NIH-PA Author Manuscript

Kask K, Jerecic J, Zamanillo D, Wilbertz J, Sprengel R, Seeburg PH. Developmental profile of kainate receptor subunit KA1 revealed by Cre expression in YAC transgenic mice. Brain Res 2000;876:55–61. [PubMed: 10973593]

Kwon HB, Castillo PE. Role of glutamate autoreceptors at hippocampal mossy fiber synapses. Neuron 2008;60:1082–1094. [PubMed: 19109913]

Lauri SE, Bortolotto ZA, Bleakman D, Ornstein PL, Lodge D, Isaac JT, Collingridge GL. A critical role of a facilitatory presynaptic kainate receptor in mossy fiber LTP. Neuron 2001;32:697–709. [PubMed: 11719209]

Melyan Z, Lancaster B, Wheal HV. Metabotropic regulation of intrinsic excitability by synaptic activation of kainate receptors. J Neurosci 2004;24:4530–4534. [PubMed: 15140923]

Melyan Z, Wheal HV, Lancaster B. Metabotropic-mediated kainate receptor regulation of I_{sAHP} and excitability in pyramidal cells. Neuron 2002;34:107–114. [PubMed: 11931745]

Mulle C, Sailer A, Perez-Otano I, Dickinson-Anson H, Castillo PE, Bureau I, Maron C, Gage FH, Mann JR, Bettler B, Heinemann SF. Altered synaptic physiology and reduced susceptibility to kainate-induced seizures in GluR6-deficient mice. Nature 1998;392:601–605. [PubMed: 9580260]

Mulle C, Sailer A, Swanson GT, Brana C, O'Gorman S, Bettler B, Heinemann SF. Subunit composition of kainate receptors in hippocampal interneurons. Neuron 2000;28:475–484. [PubMed: 11144357]

O'Gorman S, Dagenais NA, Qian M, Marchuk Y. Protamine-Cre recombinase transgenes efficiently recombine target sequences in the male germ line of mice, but not in embryonic stem cells. Proc Natl Acad Sci U S A 1997;94:14602–14607. [PubMed: 9405659]

Petralia RS, Wenthold RJ. Immunocytochemistry of NMDA receptors. Methods Mol Biol 1999;128:73–92. [PubMed: 10320974]

Pinheiro P, Mulle C. Kainate receptors. Cell Tissue Res 2006;326:457–482. [PubMed: 16847640]

Pinheiro PS, Mulle C. Presynaptic glutamate receptors: physiological functions and mechanisms of action. Nat Rev Neurosci 2008;9:423–436. [PubMed: 18464791]

Pinheiro PS, Perrais D, Coussen F, Barhanin J, Bettler B, Mann JR, Malva JO, Heinemann SF, Mulle C. GluR7 is an essential subunit of presynaptic kainate autoreceptors at hippocampal mossy fiber synapses. Proc Natl Acad Sci U S A 2007;104:12181–12186. [PubMed: 17620617]

Rodriguez-Moreno A, Lerma J. Kainate receptor modulation of GABA release involves a metabotropic function. Neuron 1998;20:1211–1218. [PubMed: 9655508]

Rodriguez-Moreno A, Sihra TS. Kainate receptors with a metabotropic modus operandi. Trends Neurosci 2007;30:630–637. [PubMed: 17981346]

Ruiz A, Sachidhanandam S, Utvik JK, Coussen F, Mulle C. Distinct subunits in heteromeric kainate receptors mediate ionotropic and metabotropic function at hippocampal mossy fiber synapses. J Neurosci 2005;25:11710–11718. [PubMed: 16354929]

Schmitz D, Frerking M, Nicoll RA. Synaptic activation of presynaptic kainate receptors on hippocampal mossy fiber synapses. Neuron 2000;27:327–338. [PubMed: 10985352]

Schmitz D, Mellor J, Nicoll RA. Presynaptic kainate receptor mediation of frequency facilitation at hippocampal mossy fiber synapses. Science 2001;291:1972–1976. [PubMed: 11239159]

Scott R, Lalic T, Kullmann DM, Capogna M, Rusakov DA. Target-cell specificity of kainate autoreceptor and Ca^{2+}-store-dependent short-term plasticity at hippocampal mossy fiber synapses. J Neurosci 2008;28:13139–13149. [PubMed: 19052205]

Swanson GT, Gereau R. W. t. Green T, Heinemann SF. Identification of amino acid residues that control functional behavior in GluR5 and GluR6 kainate receptors. Neuron 1997;19:913–926. [PubMed: 9354337]

Thomas-Crusells J, Vieira A, Saarma M, Rivera C. A novel method for monitoring surface membrane trafficking on hippocampal acute slice preparation. J Neurosci Methods 2003;125:159–166. [PubMed: 12763242]

Vignes M, Collingridge GL. The synaptic activation of kainate receptors. Nature 1997;388:179–182. [PubMed: 9217158]

Werner P, Voigt M, Keinanen K, Wisden W, Seeburg PH. Cloning of a putative high-affinity kainate receptor expressed predominantly in hippocampal CA3 cells. Nature 1991;351:742–744. [PubMed: 1648176]

NIH-PA Author Manuscript

NIH-PA Author Manuscript

NIH-PA Author Manuscript

Westbrook GL, Lothman EW. Cellular and synaptic basis of kainic acid-induced hippocampal epileptiform activity. Brain Res 1983;273:97–109. [PubMed: 6311348]

Wisden W, Seeburg PH. A complex mosaic of high-affinity kainate receptors in rat brain. J Neurosci 1993;13:3582–3598. [PubMed: 8393486]

Xu J, Zhu Y, Contractor A, Heinemann SF. mGluR5 has a critical role in inhibitory learning. J Neurosci 2009;29:3676–3684. [PubMed: 19321764]

NIH-PA Author Manuscript
NIH-PA Author Manuscript
NIH-PA Author Manuscript

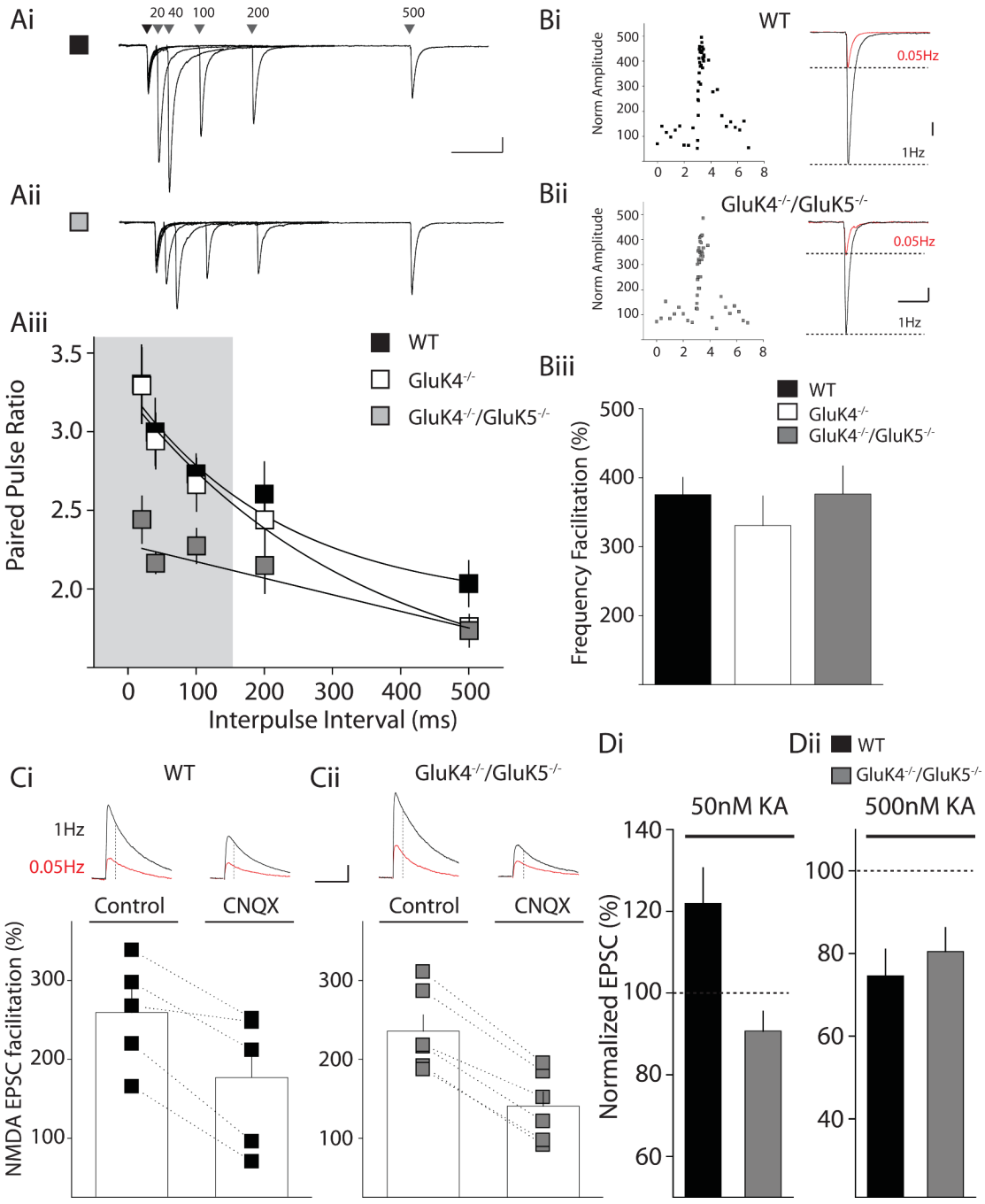

Figure 1. Paired-pulse facilitation is impaired in GluK4$^{-/-}$/GluK5$^{-/-}$ kainate receptor knockout mice but frequency facilitation is intact

(**A**) Representative examples of paired-pulse responses with intervals of 20, 40, 100, 200 and 500 ms in WT (**Ai**) and GluK4$^{-/-}$/GluK5$^{-/-}$ (**Aii**) mice. Calibration: 200pA, 100ms (**Aiii**) Grouped data of paired-pulse ratios for WT (black), GluK4$^{-/-}$ (white) and GluK4$^{-/-}$/GluK5$^{-/-}$ mice (grey). Shaded region indicates significant differences between WT and GluK4$^{-/-}$/GluK5$^{-/-}$ paired-pulse facilitation values ($p < 0.05$). (**B**) Frequency facilitation in WT (**Bi**) and GluK4$^{-/-}$/GluK5$^{-/-}$ mice (**Bii**). Left panels in Bi & Bii show the timecourse of a single recording, illustrating facilitation of mossy fiber responses when stimulation frequency is increased from 0.05 Hz to1 Hz stimulation. Right panels in Bi and Bii show example

NIH-PA Author Manuscript

NIH-PA Author Manuscript

NIH-PA Author Manuscript

responses in CA3 pyramidal neurons from WT and GluK4$^{-/-}$/GluK5$^{-/-}$ mice to 0.05 Hz or 1 Hz mossy fiber stimulation. Calibration: WT 200pA, 50ms; GluK4$^{-/-}$/GluK5$^{-/-}$ 100pA, 50ms (**Biii**) Grouped data from all frequency facilitation recordings for WT (black), GluK4$^{-/-}$ (white) and GluK4$^{-/-}$/GluK5$^{-/-}$ (grey) mice. (**C**) Frequency facilitation of the NMDA EPSC in WT (**Ci**) and GluK4$^{-/-}$/GluK5$^{-/-}$ mice (**Cii**). Representative mossy fiber EPSCs recorded at +40mV are shown in the top panels. The amplitude of the NMDA receptor component was measured 30ms after the onset of the mixed AMPA/NMDA EPSC (see methods). Bottom panel shows frequency facilitation in all recordings during control period or after application of the AMPA/kainate receptor antagonist CNQX (50 μM). In WT and GluK4$^{-/-}$/GluK5$^{-/-}$ mice frequency facilitation at 1Hz of the NMDA component of the mossy fiber EPSC was significantly reduced in CNQX. Calibration 100pA, 100ms (**Di**) Agonist-induced facilitation of mossy fiber EPSCs. 50 nM kainate significantly enhanced the mossy fiber EPSC in WT mice but had no effect in GluK4$^{-/-}$/GluK5$^{-/-}$ mice. (**Dii**) Agonist-induced depression of mossy fiber EPSCs. 500 nM kainate significantly reduced the mossy fiber EPSC amplitude in WT and GluK4$^{-/-}$/GluK5$^{-/-}$ mice.

NIH-PA Author Manuscript
NIH-PA Author Manuscript
NIH-PA Author Manuscript

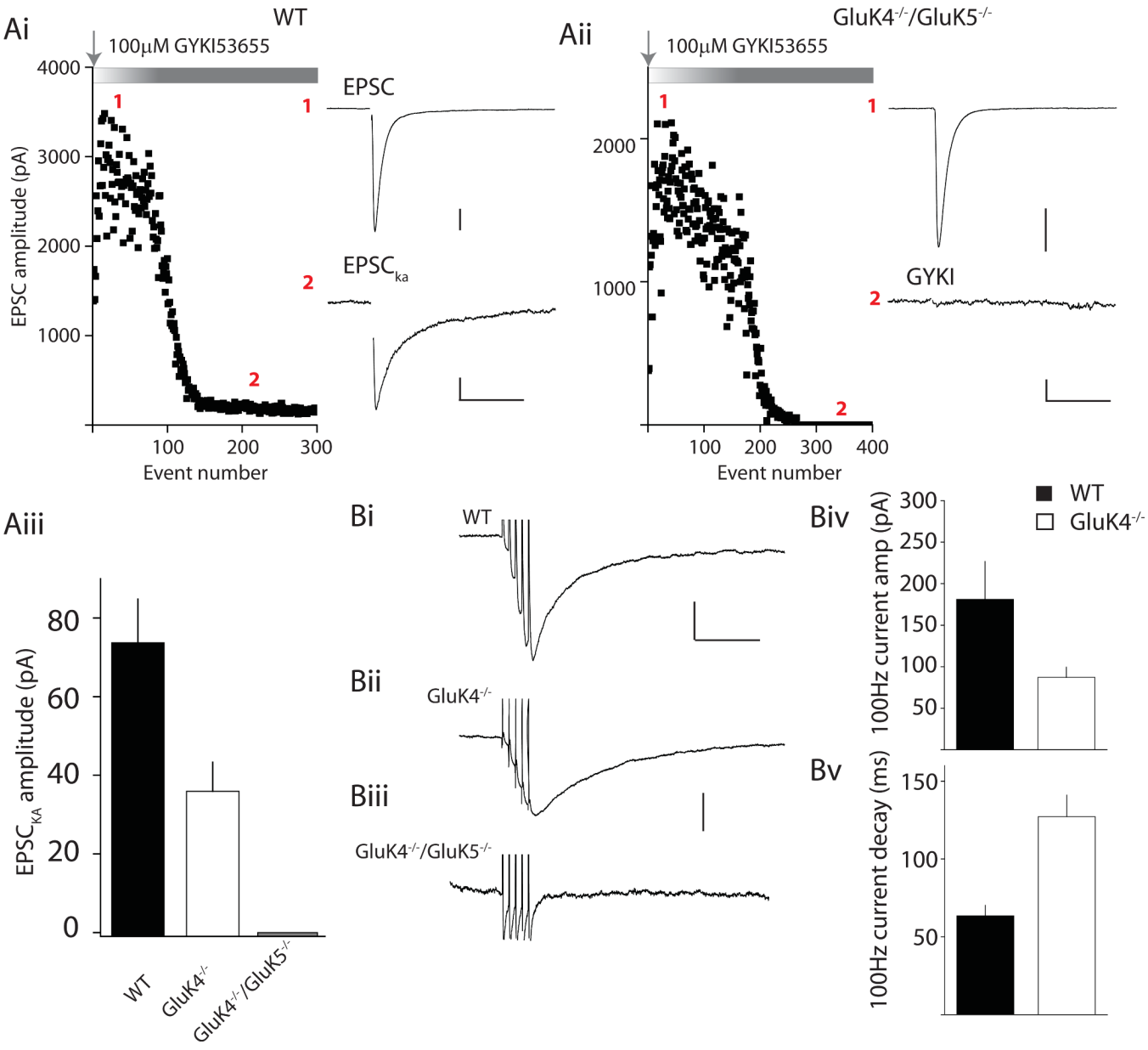

Figure 2. Mossy fiber EPSC$_{KA}$ is compromised in GluK4$^{-/-}$ and absent in double GluK4$^{-/-}$/GluK5$^{-/-}$ mice

(**Ai**) Representative experiment using single mossy fiber stimulation in wildtype mice showing block by AMPA receptors antagonist (GYKI 53655) of the majority of the mossy fiber EPSC (1). The remaining GYKI-resistant component is the slow kainate mediate component (EPSC$_{KA}$) (2) Calibration: (1) 500pA, 50ms; (2) 50pA, 50ms (**Aii**) Representative experiment using single mossy fiber stimulation in GluK4$^{-/-}$/GluK5$^{-/-}$ mice. GYKI 53655 fully blocks the mossy fiber EPSC Calibration: (1) 500pA, 50ms; (2) 50pA, 50ms (**Aiii**) Grouped data from all recordings summarizing amplitudes of EPSC$_{KA}$ recorded from WT (black), GluK4$^{-/-}$ (white) and GluK4$^{-/-}$/GluK5$^{-/-}$ (grey). (**Bi-iii**) Representative traces showing mossy fiber EPSC$_{KA}$ elicited with short trains of stimulation (5 stimuli, 100Hz) from WT, GluK4$^{-/-}$ and GluK4$^{-/-}$/GluK5$^{-/-}$ mice. Again no EPSC$_{KA}$ is observed under these conditions in double knockout mice. Calibration: (Bi) 100pA, 100ms; (Bii&iii) 50pA, 100ms (**Biv**) Grouped data

for mean $EPSC_{KA}$ current amplitudes in WT and GluK4$^{-/-}$ mice (**Bv**) Grouped data for current decay in WT and GluK4$^{-/-}$ mice.

NIH-PA Author Manuscript
NIH-PA Author Manuscript
NIH-PA Author Manuscript

NIH-PA Author Manuscript
NIH-PA Author Manuscript
NIH-PA Author Manuscript

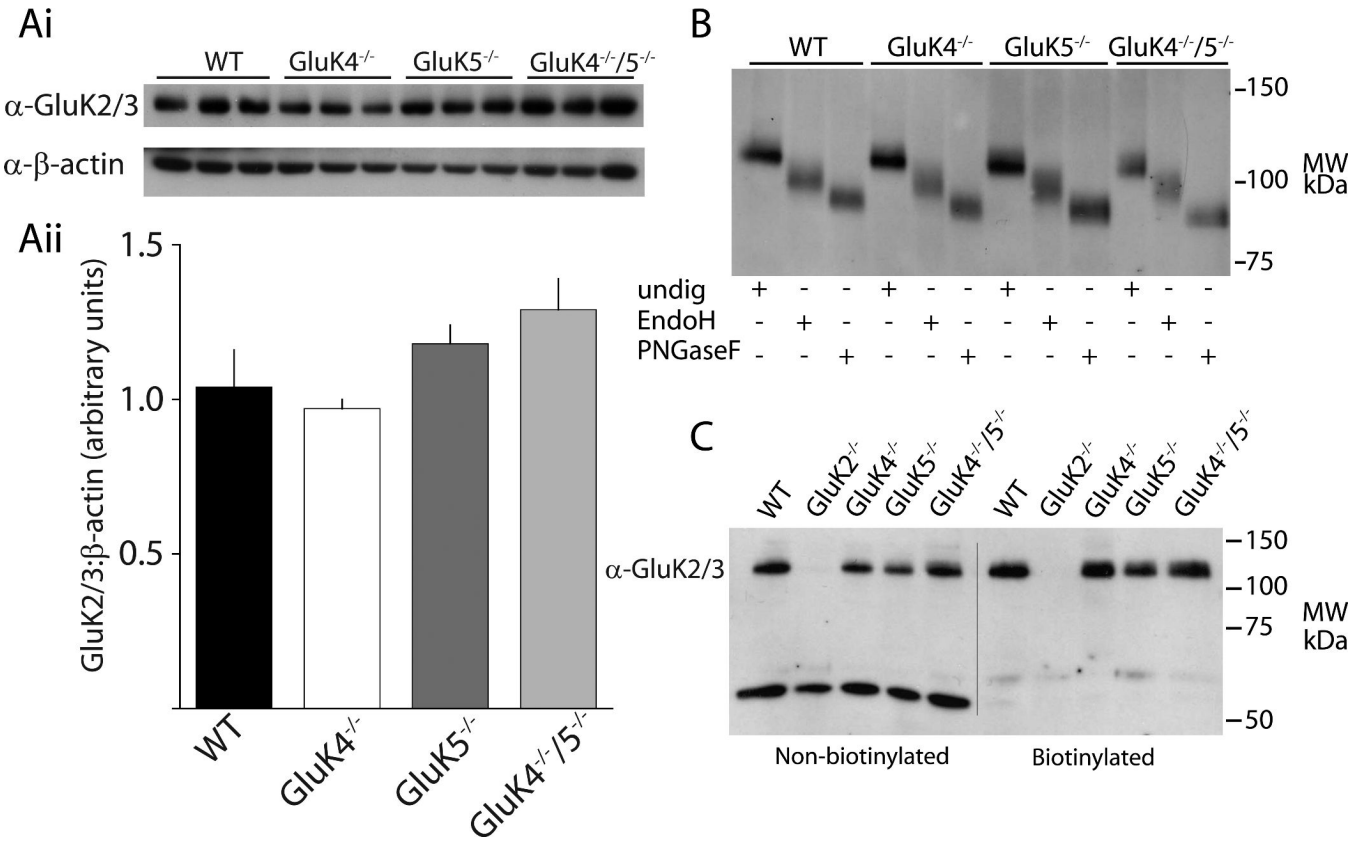

Figure 3. Biochemical analyses of principal subunits indicate no major alterations in GluK2/3 expression or processing in high-affinity subunit knockout mice

(**Ai**) Representative Western blot analysis of GluK2/3 protein in knockout mice. Protein samples were run from whole homogenate hippocampal extracts from each of the mice. (**Aii**) Quantification of Western blots. GluK2/3 expression was normalized to β-actin expression. (**B**) Representative example gel from Endo H assay. Cleavage of sugars by Endo H and PNGase F demonstrated equivalent shifts in GluK2/3 protein bands across genotypes, indicating normal glycolytic processing of GluK2/3 in knockout mice. (**C**) Representative surface biotinylation experiment. No detectable difference in the amount of surface GluK2/3 protein was observed in any of the knockout mice. Control experiments in GluK2$^{-/-}$ mice confirmed that almost all the protein detected by α-GluK2/3 in hippocampus is GluK2.

NIH-PA Author Manuscript
NIH-PA Author Manuscript
NIH-PA Author Manuscript

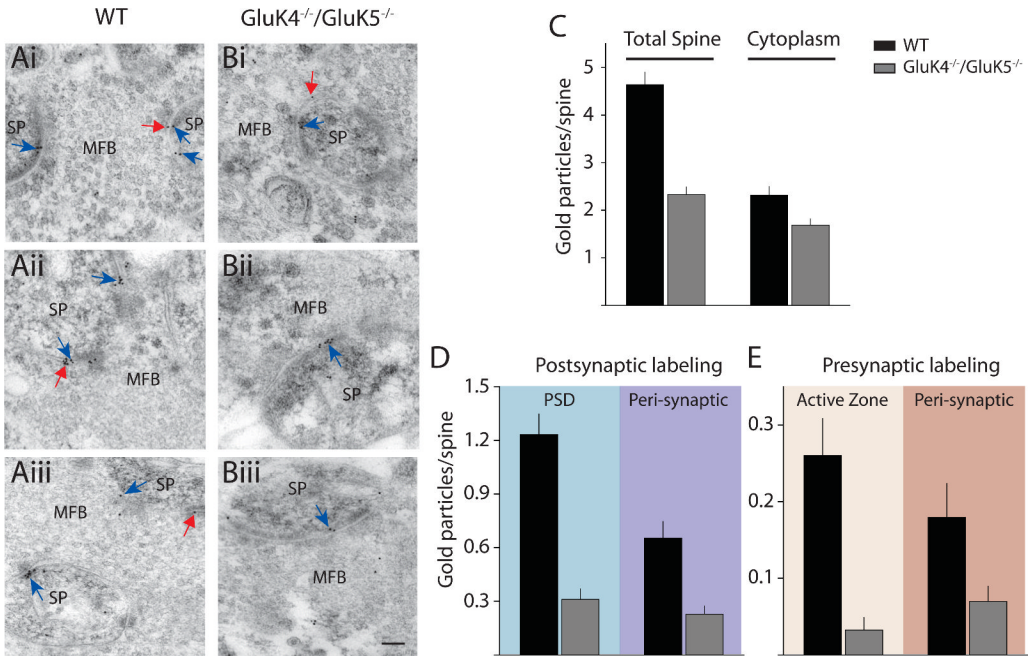

Figure 4. Immunogold EM demonstrates a large reduction in pre- and postsynaptic kainate receptor in GluK4$^{-/-}$/GluK5$^{-/-}$ mice

(**Ai-iii**) Representative electron micrographs showing mossy fiber boutons (MFB) and thorny excrescence spines (SP) from WT mice labeled with gold particles for GluK2/3. Postsynaptic labeling is indicated by blue arrows and presynaptic labeling is indicated by red arrows. (**Bi-iii**) Representative electron micrographs from GluK4$^{-/-}$/GluK5$^{-/-}$ mice. Calibration for all micrographs: 100 nm (**C**) Quantification of gold particles in spine profile depicting total spine membrane gold and cytoplasmic localized particles. (**D**) Quantification of labeling in postsynaptic spines in WT (black) and knockout (grey) mice. Gold was quantified in the PSD or in peri-synaptic regions. (**E**) Quantification of labeling on presynaptic MFBs. Gold was quantified in the active zones or distal to the release sites. WT (black) and GluK4$^{-/-}$/GluK5$^{-/-}$ (grey).

NIH-PA Author Manuscript

NIH-PA Author Manuscript

NIH-PA Author Manuscript

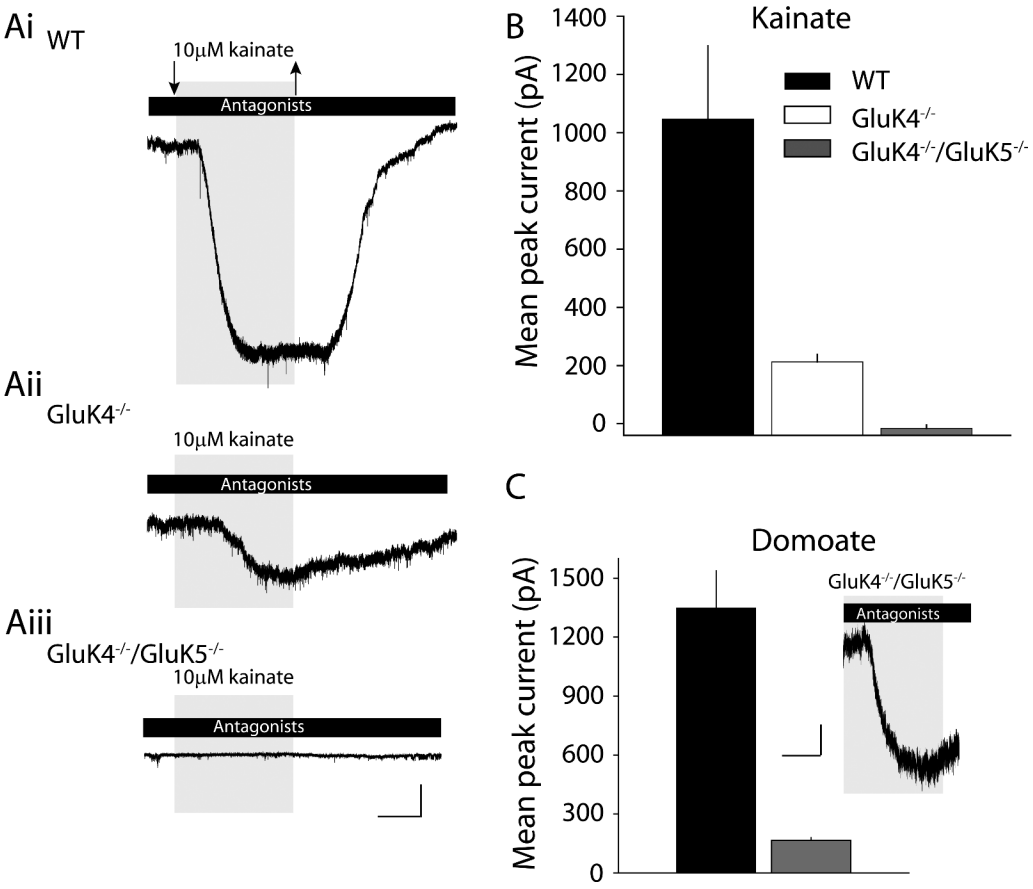

Figure 5. Agonist-induced kainate receptor mediated current in high-affinity kainate receptor knockout mice

(**Ai-iii**) Representative examples of whole-cell currents elicited by kainate (10 μM) application in the presence of AMPA, $GABA_A$ and NMDA receptor antagonists. Large inward current is observed in WT mice, whereas significantly smaller responses are observed in GluK4$^{-/-}$ mice. In double knockout mice no kainate elicited currents were observed. Calibration: 100pA, 100s. (**B**) Grouped data from all recordings depicting the mean current amplitudes elicited by kainate in CA3 pyramidal neurons in each of the mice. (**C**) Grouped data from recordings in which domoate (10 μM) was used as an agonist. This agonist elicited a response in double knockout mice which was much reduced compared to those in WT recordings. Inset is a representative example of a domoate-elicited inward current in a CA3 pyramidal neuron from GluK4$^{-/-}$/GluK5$^{-/-}$ mouse. Calibration: 50pA, 100s.

NIH-PA Author Manuscript

NIH-PA Author Manuscript

NIH-PA Author Manuscript

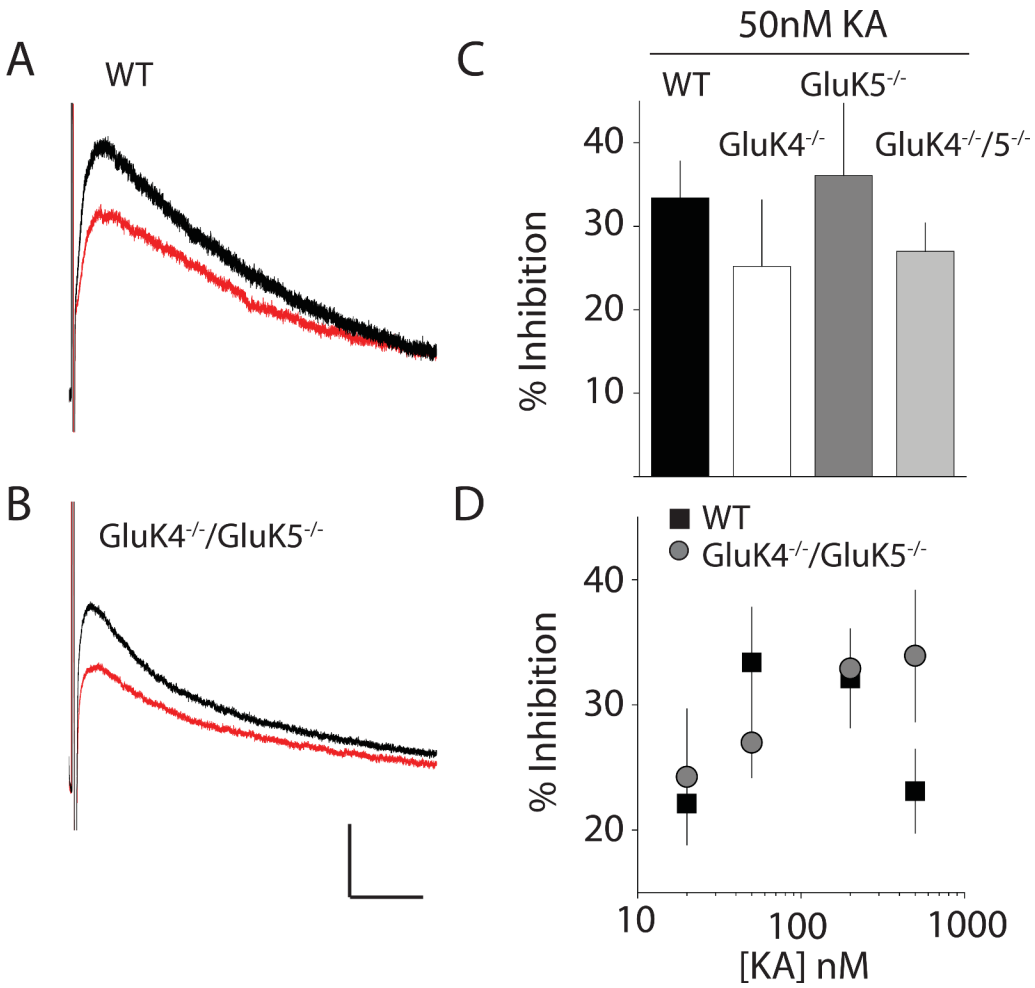

Figure 6. Kainate receptor-mediated inhibition of I_{sAHP} is intact in high-affinity kainate receptor knockout mice

(**A**) Representative I_{sAHP} traces elicited by brief depolarization (80ms, 50mV) of CA3 pyramidal neurons in WT mice. Example I_{sAHP} is shown during control period (black) and after kainate receptor-mediated inhibition (red). (**B**) Representative I_{sAHP} traces in GluK4$^{-/-}$/GluK5$^{-/-}$ mice before (black) and after (red) inhibition with 50nM kainate. Calibration 50pA, 2s (**C**) Grouped data from all recordings in which 50nM kainate was applied to inhibit I_{sAHP}. (**D**) I_{sAHP} inhibition in WT (black) and GluK4$^{-/-}$/GluK5$^{-/-}$ mice (grey) produced by several concentrations of kainic acid.